

Predictive Reconstruction of the Mitochondrial Iron-Sulfur Cluster Assembly Metabolism. II. Role of Glutaredoxin Grx5

Rui Alves,^{1,2*} Enrique Herrero,¹ and Albert Sorribas¹

¹Departament de Ciències Mèdiques Bàsiques, Universitat de Lleida, Lleida, Spain

²Biomedical Engineering Department, UC Davis, Davis, California

ABSTRACT Grx5 is a *Saccharomyces cerevisiae* glutaredoxin involved in iron-sulfur cluster (FeSC) biogenesis. Previous work suggests that Grx5 is involved in regulating protein cysteine glutathionylation, prompting several questions about the systemic role of Grx5. First, is the regulation of mixed protein-glutathione disulfide bridges in FeSC biosynthetic proteins by Grx5 sufficient to account for the observed phenotypes of the $\Delta grx5$ mutants? If so, does Grx5 regulate the oxidation state of mixed protein-glutathione disulfide bridges in FeSC biogenesis in general? Alternatively, can the $\Delta grx5$ mutant phenotypes be explained if Grx5 acts on just one or a few of the FeSC biogenesis proteins?

In the first part of this article, we address these questions by building and analyzing a mathematical model of FeSC biosynthesis. We show that, independent of the tested parameter values, the dynamic behavior observed in cells depleted of Grx5 can only be qualitatively reproduced if Grx5 acts by regulating the initial assembly of FeSC in scaffold proteins. This can be achieved by acting on the cysteine desulfurase (Nfs1) activity and/or on scaffold functionality.

In the second part of this article, we use structural bioinformatics methods to evaluate the possibility of interaction between Grx5 and proteins involved in FeSC biogenesis. Based on such methods, our results indicate that the proteins with which Grx5 is more likely to interact are consistent with the kinetic modeling results.

Thus, our theoretical studies, combined with known Grx5 biochemistry, suggest that Grx5 acts on FeSC biosynthesis by regulating the redox state of important cysteine residues in Nfs1 and/or in the scaffold proteins where FeSC initially assemble. *Proteins* 2004;57:481–492. © 2004 Wiley-Liss, Inc.

Key words: kinetic modeling; metabolic reconstruction; systemic biology; structural modeling

INTRODUCTION

Assembly of iron-sulfur clusters (FeSC), which are important cofactors in proteins, is a complex process that has not been completely characterized on a molecular level. Genetic and biochemical evidence shows that a set of proteins is involved in the proper function of FeSC-dependent cellular activity.¹ Proteins involved in FeSC biogenesis in

Saccharomyces cerevisiae include Grx5,² Ssq1,^{3–6} Jac1,^{3–7} Atm1,^{8,9} Nfu1,^{5,7,10} Yah1,¹¹ Arh1,¹² Isu1-2,^{5,7,13} Isa1-2,^{14–16} Nfs1,^{9,17} Yfh1^{18,19} and Erv1.²⁰ This series of articles aims to find the most likely systemic roles of some of these proteins by combining available information in the literature with the use of different theoretical methods and bioinformatics tools. In a previous article, we investigated the roles of the ferredoxin–ferredoxin reductase pair, Arh1 and Yah1.²¹ The results presented in that paper provided an example of how structural bioinformatics tools and kinetic modeling can be combined to perform systems analysis. Using the same approach, in this paper we investigate the role of glutaredoxin Grx5.^{22,23}

Glutaredoxins are small proteins with thiolreductase activity, that regulate the redox state of protein cysteine residues by using reduced glutathione (GSH) as an electron donor.^{24–26} Recent work has shown that Grx5 can reduce mixed protein disulfides, catalyzing the reaction $P - SS - G + GSH \leftrightarrow P - SH + GS - SG$.^{22,23} As is the case with the other proteins involved in FeSC biogenesis, the role of Grx5 is unclear. The $\Delta grx5$ mutants accumulate mitochondrial iron and show defects in FeSC-dependent protein activity.^{22,23} Is the regulation of mixed protein-glutathione disulfide bridges by Grx5 sufficient to account for the observed phenotypes of the $\Delta grx5$ mutants? If so, is Grx5 a general-purpose mixed protein-glutathione disulfide bridge formation regulator in FeSC biogenesis? Alternatively, can the $\Delta grx5$ mutant phenotypes be explained if Grx5 acts on just one or a few of the FeSC biogenesis proteins?

We address these questions by extending a previous mathematical model of mitochondrial FeSC biogenesis²¹ to include alternative possible modes of Grx5 action. This extension considers protein inactivation/recovery by glutathionylation/deglutathionylation of protein cysteinyl residues, regulated by Grx5. We test the effect of depleting Grx5 on the dynamic behavior of the network model when Grx5 is considered to regulate the glutathionylation/deglutathionylation of each FeSC biogenesis protein in the

The Supplementary Materials referred to in this article can be found at <http://www.interscience.wiley.com/jpages/0887-3585/suppmat/index.html>

Correspondence to: Rui Alves, Departament de Ciències Mèdiques Bàsiques, Universitat de Lleida, Av. Rovira Roure 44, 25198 Lleida, Spain. E-mail: ralves@cmb.udl.es, or ralves@ucdavis.edu.

Received 12 February 2004; Revised 10 May 2004; Accepted 10 May 2004

Published online 29 July 2004 in Wiley InterScience (www.interscience.wiley.com). DOI: 10.1002/prot.20228

TABLE I. Minimal Reaction Model for FeSC Biosynthesis in *S. cerevisiae*

Reaction ^a	Rate and modifiers ^b	Reaction ^a	Rate and modifiers ^b
IsuFe2S2 → Isu + 2Fe	$v1 = \alpha_1 IsuFe_2S_2^{f11}$	AY1 → AY1_I	$v15 = \alpha_{15} AY1^{f151}$
IsuFe2S2 + Apo_P1 → P1 + Isu	$v2 = \alpha_2 IsuFe_2S_2^{f21} Apo P1^{f22} (AY1)^{f23}$	→ Fe	$v16 = \alpha_{16}$
IsuFe2S2 + Apo_AY1 → Isu + AY1	$v3 = \alpha_3 IsuFe_2S_2^{f31} Apo AY1^{f32} (AY1)^{f33}$	Heme_Fe → Fe + Heme	$v17 =$
IsuFe4S4 + Apo_P2 → P2 + Isu	$v4 = \alpha_4 IsuFe_4S_4^{f41} Apo P2^{f42} (AY1)^{f43}$	Fe →	$v18 = \alpha_{18} Fe^{f181}$
Isu + 2 Fe → IsuFe2S2	$v5 = \alpha_5 Isu^{f51} Fe^{f52} (Nfs_1)^{f53} AY1^{f54}$	Heme + Fe → Heme_Fe	$v19 = \alpha_{19} Fe^{f191} Heme^{f192}$
IsuFe2S2 + 2 Fe → IsuFe4S4	$v6 = \alpha_6 IsuFe_2S_2^{f61} Fe^{f62} (Nfs_1)^{f63} AY1^{f64}$	→ Heme	$v20 = \alpha_{20} (AY1)^{f201}$
IsuFe4S4 → IsuFe2S2 + 2 Fe	$v7 = \alpha_7 IsuFe_4S_4^{f71}$	Heme →	$v21 = \alpha_{21} Heme^{f211}$
P2_I → Apo_P2 + 4 Fe	$v8 = \alpha_8 P2_I^{f81}$	IsuFe2S2 + Apo_P2 → Isu + P2Fe2S2	$v22 = \alpha_{22} IsuFe_2S_2^{f221} Apo P2^{f222} (AY1)^{f223}$
P2_I → P2	$v9 = \alpha_9 P2_I^{f91} (Nfs_1)^{f92} AY1^{f93}$	IsuFe2S2 + P2Fe2S2 → Isu + P2	$v23 = \alpha_{23} IsuFe_2S_2^{f231} P2Fe_2S_2^{f232} (AY1)^{f233}$
P2 → P2_I	$v10 = \alpha_{10} P2^{f101}$	P2Fe2S2 → Apo_P2 + 2 Fe	$v24 = \alpha_{24} P2Fe_2S_2^{f241}$
PI_I → Apo_P1 + 2Fe	$v11 = \alpha_{11} P1_I^{f111}$	IsuFe4S4 → Isu + 4 Fe	$v25 = \alpha_{25} IsuFe_4S_4^{f251}$
PI_I → PI	$v12 = \alpha_{12} P1_I^{f121} (Nfs_1)^{f122} AY1^{f123}$	IsuFe2S2 → Isu + FeSC _{cytoplasm}	$v26 = \alpha_{26} IsuFe_2S_2^{f261} (AY1)^{f262}$
P1 → P1_1	$v13 = \alpha_{13} P1^{f131}$	IsuFe4S4 → Isu + FeSC _{cytoplasm}	$v27 = \alpha_{27} IsuFe_4S_4^{f271} (AY1)^{f272}$
AY1_I → AY1	$v14 = \alpha_{14} AY1_I^{f141} (Nfs_1)^{f142} AY1^{f143}$	AY1_I → Apo_AY1 + 2 Fe	$v28 = \alpha_{28} AY1_I^{f281}$
Isu → IsuGS	$v29 = \alpha_{29} Isu^{f291}$	Apo_P2 → P2GS	$v35 = \alpha_{35} Apo P2^{f351}$
IsuGS → Isu	$v30 = \alpha_{30} IsuGS^{f301} ([Grx5])^{f302}$	P2GS → Apo_P2	$v36 = \alpha_{36} P2GS^{f361} ([Grx5])^{f362}$
Apo_AY1 → AY1GS	$v31 = \alpha_{31} Apo AY1^{f311}$	Nfs1 → Nfs1GS	$v37 = \alpha_{37} Nfs1^{f371}$
AY1GS → Apo_AY1	$v32 = \alpha_{32} YaIGS^{f321} ([Grx5])^{f322}$	Nfs1GS → Nfs1	$v38 = \alpha_{38} Nfs1^{f381} ([Grx5])^{f382}$
Apo_P1 → P1GS	$v33 = \alpha_{33} Apo P1^{f331}$	Nfs1 + Isu → Nfs1_Isu	$v39 = \alpha_{39} Nfs1^{f391} Isu^{f392}$
PIGS → Apo_P1	$v34 = \alpha_{34} PIGS^{f341} ([Grx5])^{f342}$	Nfs1_Isu → Nfs1 + Isu	$v40 = \alpha_{40} Nfs1_Isu^{f401} ([Grx5])^{f402}$
		Grx5 →	$v41 = \alpha_{41} Grx5^{f411}$

^aIsu-scaffold for initial FeSC assembly; IsuFe2S2, IsuFe4S4-scaffold with an Fe2S2 and an Fe4S4 FeSC cluster assembled, respectively; Fe-mitochondrial iron; P1-generic enzyme needing a Fe2S2 FeSC to be functional; P2-generic enzyme needing a Fe4S4 FeSC to be functional; AY1-electron donor (either Arh1 or Yah1, depending on the experiment; see text for an explanation); Apo_P1, Apo_P2, Apo_AY1-apo forms of P1, P2 and AY1, respectively; P1_I, P2_I, AY1_I-P1, P2 and AY1 forms with a damaged and repairable FeSC; P2Fe2S2-P2 enzyme with an intermediate Fe2S2 cluster assembled; Heme-heme molecules synthesized in the mitochondrial matrix; Heme; Fe-heme molecules with iron. IsuGS, AY1GS, P1GS, P2GS and Nfs1GS-inactive forms of the proteins, whose activity can be recovered by action of Grx5; Nfs1_Isu-dead-end complex formed between Nfs1 and scaffold proteins which can be recovered by the action of Grx5.

^bSpecies in parentheses and brackets in the equations are not represented in the flux diagram because they contribute to the catalysis of the reaction but are neither produced nor consumed in the reaction; bracketed species represent the scrutinized role of Grx5.

cently, it has been shown that $\Delta grx5$ mutant cells accumulate FeSC in scaffold proteins.³⁰

We will use these results to challenge our models and test the different hypotheses about the role of Grx5. To reproduce these experiments in our models, we normalized the Grx5 activity and introduced a sink flux that depletes this activity, without introducing a source flux. This reproduced the published experiments in the sense that *GRX5* expression was turned off and Grx5 was then degraded in the cell.³¹ We then computed the relative amounts of FeSC-dependent proteins containing FeSC (P1, P2 and AY1 in Table I), at various kinetic order values and at various ratios for the fluxes of the different processes shown in Table I. Details about our methods for scanning the parameters are given in the appendix.

The various modes of Grx5 action and the respective admissible values for the rate constants are presented in Table II. The admissible parameter values for the Grx5 kinetic orders, which were scanned for each of the modes, are shown in Table III. The total amount of each protein, except for Grx5 remains constant throughout the experiments. For example, the total amounts of 2Fe-2S-dependent enzymes, represented by P1 (P1 + Apo P1 + P1_I + P1GS), and 4Fe-4S-dependent enzymes, represented by P2 (P2 + Apo P2 + P2_I + P2GS), are considered to be

constant. This assumption is justified because protein synthesis and degradation usually takes place on a time scale (hours to days) that is orders of magnitude lower than that of FeSC turnover (minutes to hours). For example, FeSC-dependent enzyme levels are approximately constant throughout the entire experimental procedure described by Rodriguez-Manzanique and coworkers.²

Structural Modeling

Once we eliminated those modes of action for Grx5 that do not reproduce the experimentally observed dynamic behavior of the FeSC assembly system, we were left with a few possible modes of interaction between Grx5 and FeSC assembly proteins. To further support these interactions, we analyzed the structures of the proteins involved that were predicted to form the most likely complexes. If a target protein with an undetermined structure has sufficient sequence homology to another protein of known structure, the latter protein can be used as a template to model the target sequence in three-dimensional space.^{32,33} We used this well-established technique, known as homology modeling, to predict the structure of Nfs1. We locally aligned target and template sequences using the following programs: 3DJIGSAW,³⁴ SWISSMODEL,^{35,36} BONSAI,³⁷

TABLE II. Experiments to Determine Effect of Depleting Grx5 on Dynamic Behavior of Network^a

Mode of Grx5 action in recovering FeSC synthesis proteins	Kinetic orders regulating each flux					
	v_{30}	v_{32}	v_{34}	v_{36}	v_{38}	v_{40}
Recovery of Isu_GS complex	$5 \geq g_{302} > 0$	$g_{322} = 0$	$g_{342} = 0$	$g_{362} = 0$	$g_{382} = 0$	$g_{402} = 0$
Recovery of AY1GS complex	$g_{302} = 0$	$5 \geq g_{322} > 0$	$g_{342} = 0$	$g_{362} = 0$	$g_{382} = 0$	$g_{402} = 0$
Recovery of P1GS	$g_{302} = 0$	$g_{322} = 0$	$5 \geq g_{342} \geq 0$	$g_{362} = 0$	$g_{382} = 0$	$g_{402} = 0$
Recovery of P2GS	$g_{302} = 0$	$g_{322} = 0$	$g_{342} = 0$	$5 \geq g_{362} \geq 0$	$g_{382} = 0$	$g_{402} = 0$
Recovery of Nfs1_GS complex	$g_{302} = 0$	$g_{322} = 0$	$g_{342} = 0$	$g_{362} = 0$	$5 \geq g_{382} > 0$	$g_{402} = 0$
Recovery of Nfs1_Isu complex	$g_{302} = 0$	$g_{322} = 0$	$g_{342} = 0$	$g_{362} = 0$	$g_{382} = 0$	$5 \geq g_{402} > 0$

^aThis table presents the parameter values for the action of Grx5 in individually recovering the activity of each of the different proteins shown in Table I. For example, when Grx5 acts exclusively to recover Isu activity, the parameter values are those of the first row. To test combinations of different modes of action, combine the entries that are not 0 from each of the corresponding rows, keeping the remaining parameter values as 0. For example, to test the dynamical behavior of the model if Grx5 acts on Isu_GS and Nfs1GS simultaneously, we use as parameter values $5 \geq g_{302} > 0$, $5 \geq g_{382} > 0$, $g_{322} = g_{342} = g_{362} = g_{402} = 0$.

TABLE III. Residue Conservation Between NifS (1 kmk.pdb template) Residues Forming Active Center or Involved in Cofactor Interaction and Nfs1^a

NifS	Nfs1
Thr94	Ala168
Thr95	Thr169
His123 ^d	His197
His124 ^d	Lys198
Ala125	Cys199
Asp200	Asp273
Ala202	Ala275
Gln203	Gln276
Ser223	Ser296
His225	His298
Lys226 ^{b,d}	Lys299
Gly253 ^c	Gly326
Ser254 ^d	Ser334
Gly277 ^c	Gly335
Thr278 ^c	Thr336
Arg359 ^d	Ser416
His362	His443
Cys364 ^d	Cys421
Arg379 ^d	Arg447

^aA best fit of the backbone between all corresponding residues has a RMS of 2.90 Å, mostly due to pairing of residues Ser254–Ser334, His364–His443 and Thr278–Thr336.

^bResidue that covalently binds the PLC cofactor.

^cResidues from the opposite monomer.

^dResidues forming the active center; The total RMSD between the backbones of these residues is 2.26 Å, mostly due to the pair Ser254–Ser334.

CLUSTAL,³⁸ ITERALIGN³⁹ and 3D-PSSM.³⁴ A consensus alignment was derived (Supplementary Figure 1).

The model used for Grx5 is a refined version of that presented by Belli and coworkers,²³ using structure file 1KTE from the Protein Data Bank (PDB) for the refinement. This PDB file has the highest sequence identity with the target sequence ($\approx 29\%$). For Nfs1 and the scaffold proteins, we used PDB template files 1KMK (the structure of the *Escherichia coli* cysteine desulfurase homologue NifS) and 1Q48 and 1R94 (structures for the *E. coli* scaffold proteins), respectively.⁴⁰ The 1KMK file was selected over other structures that have higher sequence identities with Nfs1 ($\approx 27\%$ vs. $\approx 57\%$ for 1P3W). The

reason for this choice is that 1KMK provides the structure for the loop containing the active center cysteine, a detail that is absent in the structure of other possible templates such as 1P3W. Thus, we used 1KMK as the primary template and used 1P3W and 1ECX to reconstruct loops of the Nfs1 model. The template files for the scaffold proteins were selected because their sequences had the smallest *E*-values of all candidates with known structures upon alignment to their respective target proteins. The alignments were submitted to the SWISS-MODEL and 3D-JIGSAW servers for initial structure prediction, and the resulting models were optimized using DEEVIEW^{35,36} to reconstruct small loops and rearrange clashing residues. A final full energy minimization was performed on the models using the GROMACS97 force field.⁴¹ Point mutations were introduced in the structural models using DEEVIEW,^{35,36} followed by side-chain optimization and full energy minimization of the mutants. The Arh1 and Yah1 models have been described previously.²¹

Protein Docking

Given the atomic coordinates of two proteins, docking methods search for the bound complex between them in which the shape of the two surfaces fit best.^{42,43} Protein docking experiments were conducted using GRAMM^{44–46} and Hex.⁴⁷ The GRAMM methodology is particularly appropriate for the docking of our low-resolution model structures because it scans and compares the entire protein surfaces, averaging structural details and predicting general features of the ligand–receptor complex.^{42,44–46}

RESULTS AND DISCUSSION

Dynamic Modeling Results

Minimal Network Model for Grx5 Action on Mitochondrial FeSC Metabolism

Figure 1 and Table I present a network model for FeSC assembly in the mitochondrial matrix. This is an extension of a previously published model.²¹ Please refer to this publication for details of the basic model. To investigate the contribution of Grx5, we complemented the published model according to the following hypotheses of Grx5 action.

Grx5 may act by regulating the glutathionylation state of cysteine residues in FeSC-dependent proteins.⁴⁸ Glutathionylation of cysteine residues that are involved in FeSC coordination could prevent holo-enzyme formation. The general 2Fe-2S-dependent protein P1 and 4Fe-4S dependent protein P2 were each considered to form an inactivated pool that can be reactivated by Grx5.

Grx5 may act by regulating the glutathionylation state of cysteine residues in Arh1, Yah1, scaffold or Nfs1 proteins.²² It may also be involved indirectly in regulating the formation/destruction of internal disulfide bridges in any of these proteins.²² Our model cannot distinguish between these two alternatives.

Grx5 activity capable of reducing protein–protein disulfide bridges may reduce complexes formed between different FeSC proteins. The only such case reported in the literature is between Isu and Nfs1, which forms a dead-end complex between the two proteins in the absence of iron on the scaffold dimers.⁴⁹ Grx5 may be active in reducing these bridges and returning both proteins to active duty in FeSC assembly.

These three hypotheses, based on the available biochemical information on Grx5, together with the previously derived model for FeSC assembly, define a minimal network model for us to study the action of Grx5 on mitochondrial FeSC assembly metabolism.

Dynamic Effect of Grx5 on FeSC Mitochondrial Metabolism in *Saccharomyces cerevisiae*

The experimental depletion of Arh1 or Grx5 was reproduced in our models by depleting the total amount of this protein using a decay function similar to that determined *in vivo*.³¹ This function is represented by v39 in Table I. Solving the dynamic equations of the model allows calculation of the percentage of each protein (Scaffold proteins, P1, P2 and AY1) that is in its holo form, as well as the mitochondrial iron levels. The Holo form of an FeSC-dependent protein is assumed to be proportional to the total activity of this protein. By working with normalized quantities, we determined the qualitative behavior most common to alternative network models. By changing the values for the kinetic orders of Grx5 on the different equations, we determined the dynamic behavior of the system under all biologically relevant parameter values for Grx5 action. Tables II and III describe the various kinetic experiments and explain the nomenclature for the modes of action of Grx5. Although no clear data on the mechanism or accurate estimates for the parameter values of the system exist, we used normalized quantities and the power-law formalism as a modeling framework to overcome these two concerns. Details are provided in the appendix and in the references therein. Examples of how this low-resolution modeling approach has assisted in discerning among alternative roles of proteins in different cellular networks can be found in the literature.^{50,51}

Figure 2 shows typical dynamic curves for the effect of regulating the gene expression of Grx5 about its normal value on mitochondrial iron levels and on FeSC-dependent enzyme activities. In our model, the exact basal levels of both

mitochondrial iron and FeSC-dependent enzyme activities depend on parameter values. However, both mitochondrial iron levels [Fig. 2(b)] and enzyme activities [Fig. 2(c)] are mostly unresponsive to a decrease in the level of Grx5, when Grx5 is assumed to act in regulating Arh1 or Yah1 activity, scaffold protein activity, the glutathionylation state of FeSC-dependent enzymes, or any combination of these individual modes of Grx5 action. In an opposing effect, the accumulation of FeSC in the scaffold proteins observed to occur *in vivo* upon Grx5 protein depletion³⁰ occurs with each mode of Grx5 considered in the simulations. Thus, this phenotypic characteristic cannot be used to differentiate among the different modes of Grx5 action in our model [Fig. 2(d)]. An interesting observation from our simulation is that this accumulation is likely to be a transient effect. As the depletion of Grx5 proceeds, the level of FeSC in the scaffold proteins decreases.

If Grx5 acts in regulating Nfs1 activity, we observe an effect of its depletion on FeSC-dependent enzyme activity and on mitochondrial iron accumulation that, qualitatively, is similar to what is observed experimentally [Fig. 2(d)]. Mitochondrial iron levels increase and FeSC-dependent enzyme activity decreases with depletion of Grx5. The typical shape of the time curve response is that of the curves shown in Figure 2. Typically, mitochondrial iron levels and FeSC-dependent enzyme activity respond faster to Grx5 depletion if Grx5 acts to recover a dead-end complex that forms by disulfide bridging between Nfs1 and Isu or Isa proteins in the absence of iron. However, for comparable systems, response times of this mode of action and a mode of action in which Grx5 only acts to regulate the glutathionylation state of Nfs1 are similar. Furthermore, the shape of the time response is qualitatively similar. This indicates that, as long as Grx5 acts to regulate Nfs1 activity, the experimental effects of Grx5 depletion can always be qualitatively reproduced, independent of the other modes of action of Grx5 and of parameter values. If, on the other hand, Grx5 is not considered to act in either of these two modes, experimental results cannot be qualitatively reproduced, independent of the particular parameter values considered. This strongly suggests that Nfs1 and probably also the scaffold proteins are targets for Grx5 action in FeSC assembly. To further investigate this theoretical prediction, we performed structural and protein docking studies on models of both proteins.

Structural Results ***Structural Modeling***

Because there is no known structure for Grx5, Nfs1 or the scaffold proteins, structural models for each protein were needed (Fig. 3). These models were derived either from homologous proteins (Nfs1, scaffold proteins) or from improvements upon previously studied models (Grx5²³).

Nfs1 is a cysteine desulfurase, dimeric in its biologically active form. Figure 3(b) shows a model of the Nfs1 dimer superimposed on the structure of the NifS *E. coli* enzyme. The root mean square deviation (RMSD) of the total backbone atoms between the dimers is 13.70 Å. For the individual molecules, the RMSD is 6.35 Å, after loop reconstruction (and less than 1 Å before loop reconstruction). There is sequence

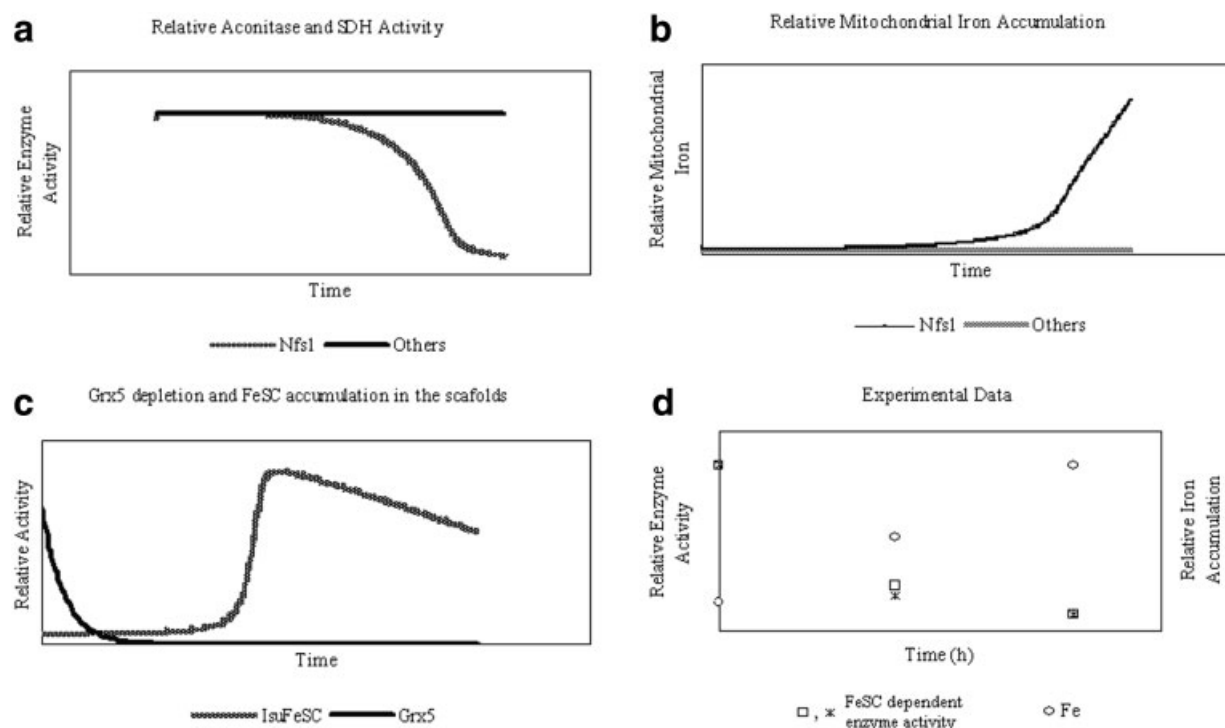


Fig. 2. Typical curves for the qualitative effect of depleting Grx5 activity in yeast cells on mitochondrial iron accumulation, and on FeSC dependent enzyme activity, represented here by succinate dehydrogenase (SDH) and aconitase. Plots are dimensionless. The Nfs1 show the typical qualitative effect when Grx5 acts to recover Nfs1 activity, and the Others curves, show the typical qualitative effect when Grx5 does not act to recover Nfs1 activity. Graphs illustrate (a) the effect of Grx5 depletion on FeSC dependent enzyme activity, (b) the effect of Grx5 depletion on the mitochondrial iron accumulation, (c) the typical depletion schedule for Grx5 in the simulations. (Also shown is a typical curve for the accumulation of FeSC in the scaffold proteins upon depletion of Grx5), (d) the re-plotting of experimental data from refs. (7–9). Because we provide typical qualitative results for the considered situations, figures do not include numbers.

and spatial conservation between several important residues of Nfs1 and the *E. coli* enzyme NifS. These are shown in Table III. Notable among these is the strong conservation between the active center residues of NifS and the putative active center residues of Nfs1. The backbone superposition of corresponding residues between the NifS active center and the putative Nfs1 active center is almost perfect, with the exception of the residue pairs Ser254^{NifS}–Ser334^{Nfs1}, His364^{NifS}–His443^{Nfs1} and Thr278^{NifS}–Thr336^{Nfs1}. Several important cofactor interacting residues are also conserved between NifS and Nfs1. The arrow in Figure 3(c) shows the putative active center cavity in one of the monomers. Cys421 is, upon sequence alignment to the bacterial enzyme, predicted to be the active center cysteine. A structural fit of the entire molecular structures superimposes the active center Cys364 from the *E. coli* enzyme with the putative active center Cys421 from Nfs1. In a high-oxidant environment, this residue is predicted to be fairly accessible to glutathionylation [Figure 3(e)]. Under such glutathionylating conditions, Nfs1 would become inactive, preventing FeSC *de novo* assembly or repair.

To obtain further support for our result and test whether Grx5 can act on Nfs1, we performed protein docking experiments between the Grx5 model and the monomer and predicted dimer of Nfs1. Analysis of the resulting data must take into account that docking methods are still far from accurate. When docking models (low resolution docking), reasonable solutions are more likely to be found in

large clusters of slightly different solutions with low energy than in the solution with the lowest energy.^{44–46} Figure 4 shows predicted dockings between Grx5 and Nfs1. The active residue of Grx5 is Cys60, which is shown to dock close to the putative Nfs1 active site, suggesting the possibility that Grx5 could regulate the glutathionylation state of the cysteine desulfurase active site. The solutions presented in Figure 4 are not the ones with the lowest energy found during the docking experiments. However, they are always within the 15 top-ranked solutions, and they represent clusters with either the most [Fig. 4(c)] or the second-most [Fig. 4(a,b)] solutions within fifty lowest-energy solutions.

Belli and coworkers²³ have studied the physiological effects of several point mutations in Grx5. Many of these mutations had little or no effect on the physiological role of Grx5, with the exception of Phe50 → Glu, Cys60 → Ser, Gly61 → Val, Gly61 → Ser, Gly115 → Val and Gly115 → Ser. Cys60 is the active center residue. We created models for each of the previously reported point mutants²³ [shown here in Suppl. Fig. 2(c)]. Our models predict that each of the reported point mutations has little effect on the surface properties of Grx5, suggesting that loss of function in Grx5 mutants may be due to effects on intra-protein interactions and/or reaction mechanisms [Suppl. Fig. 2(c)]. This is supported by the fact that, except for Phe50, all other residues are close to cysteines that have been shown to be important in Grx5 activity.^{22,23}

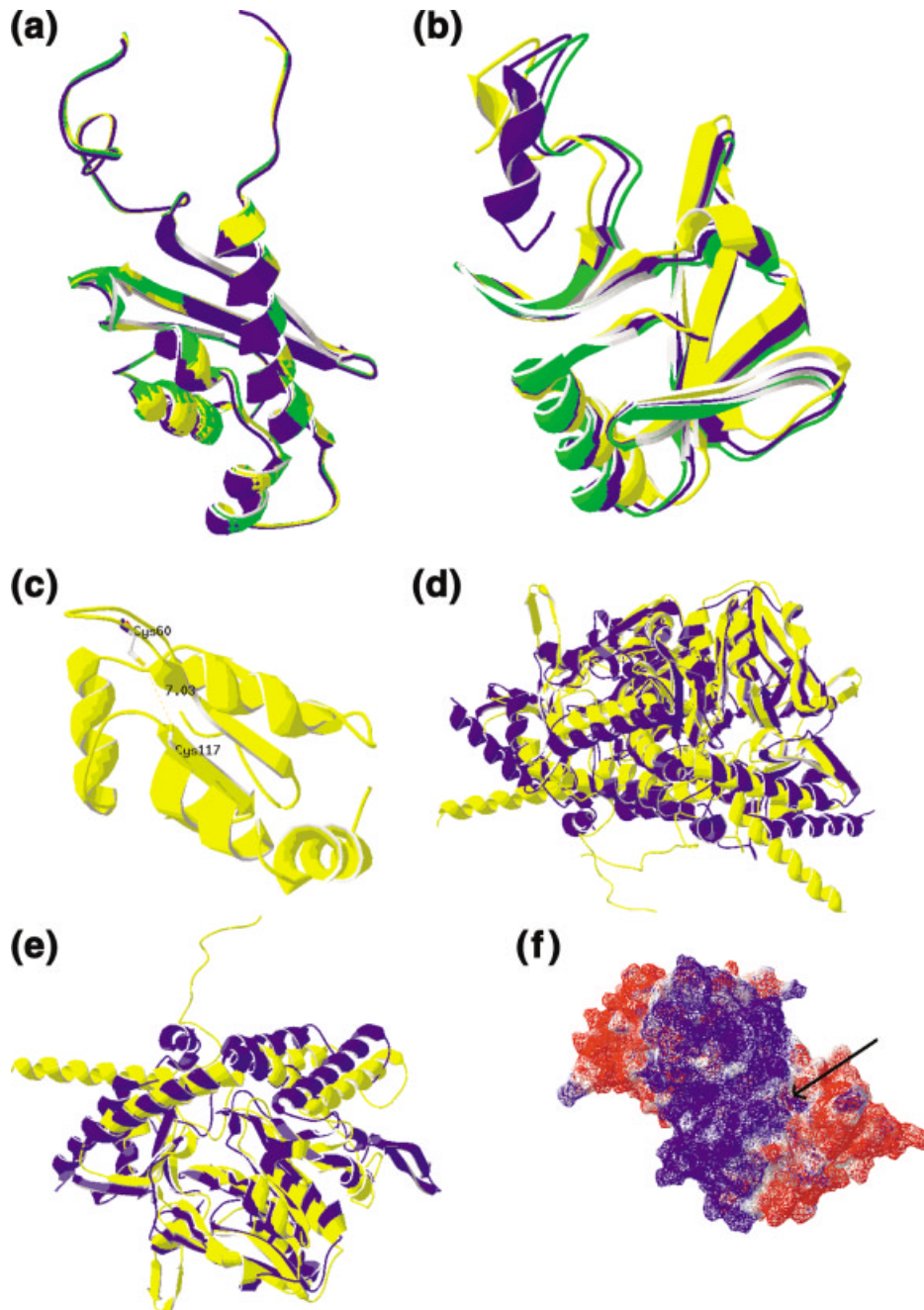


Fig. 3. Structural models for Grx5 and Nfs1. See text for details. (a) Isu1 (yellow) and Isu2 (green) models are superimposed on the template IscU protein from *E. coli* (blue). The backbone RMSD is 2.76 Å for Isu1 and 4.90 Å for Isu2. (b) Isa1 (green) and Isa2 (yellow) models are superimposed on the template IscA protein from *E. coli* (blue). The backbone RMSD is 3.52 Å for Isa1 and 2.12 Å for Isa2. (c) Model for Grx5. (d) Putative dimer of Nfs1 (yellow) is superimposed on the template dimer (blue) rebuilt from PDB file 1kmk.pdb. The RMSD of the backbone is 13.7 Å. (e) Nfs1 monomer is superimposed on the 1kmk.pdb monomer. The backbone RMSD is about 7 Å after loop reconstruction. (f) Electrostatic surface calculation for the dimer of Nfs1. The white arrow indicates the putative active site, based on sequence and structural homology to the bacterial 1kmk.pdb entry. The electrostatic potential was calculated assuming a protein dielectric constant of 4, a solvent dielectric constant of 80 Debye and a solvent ionic strength of 0.1M. Residues with a surface charge calculated Debye to be larger than 1.8 (kT) are colored blue. Residues with a surface charge calculated to be smaller than -1.8 (kT) are colored red. Remaining residues are shown in white.

To extend Belli's work and derive testable predictions to support our results, we performed *in silico* protein mutation studies. If our docking predictions are correct, a

negative Grx5 surface docks a small positive Nfs1 surface. This suggests that mutations affecting docking surface properties might disrupt the function of Grx5. Table IV

TABLE IV. Tested Point Mutations Based on Docking Complexes Between Grx5 and Nfs1^a

Grx5 Mutations	Nfs1 Mutations
Lys52 → Glu	Glu329 → Arg
Glu56 → Arg	Lys198 → Glu, Arg205 → Glu
Pro58 → Glu	Asp438 → Arg, Asp439 → Arg
Lys59 → Asp	Glu196 → Arg
Asp88 → Glu	Asn141 → Glu

^aBold Grx5 residues are most likely to disrupt the docking, based on shape and electrostatics.

shows a list of residues on the Grx5 (left column) surface that are predicted to be less than 6 Å from corresponding and oppositely charged Nfs1 residues (right column) in our predicted docking complexes. This is a distance that could allow for the formation of salt bridges between the two proteins. Mutations to one or more of the residues shown in Table IV could change electrostatic surface properties of the molecules and thus disrupt the docking, affecting Grx5 function. Studying the predicted effects of each point mutation on the surface properties of Grx5 and Nfs1 shows that most Grx5 point mutants have a slightly more negative surface charge than the wild type, without any large change in shape [Suppl. Figure 2(a)]. Because the surface of the Nfs1 dimer where Grx5 binds is predicted to have a positive charge [Suppl. Fig. 2(b)], such changes in the Grx5 surface properties should have little effect on the formation of the complex, although they could affect the reaction mechanism. The exceptions to these considerations are the Glu56 → Arg and Asp88 → Arg point mutants. These create a more positive surface charge on the Grx5 docking surface that, if our predictions are correct, could disrupt its docking with Nfs1. We have tested these predictions by creating *in silico* mutated proteins and performing docking experiments with the different mutant proteins presented in Table IV.

We docked the mutant Grx5 proteins to wild-type Nfs1 dimers and the mutant Nfs1 dimers to wild-type Grx5. We found that the Glu56 → Arg mutation in Grx5 has little effect on the rank and clustering of the complexes predicted to form between Grx5 and Nfs1 by the docking programs. On the other hand, the Asp88 → Arg mutation has a larger effect on these parameters. An analysis of the 100 best solutions for the predicted docking between Nfs1 (with mutations Asn141 → Glu and Lys198 → Glu) and the Grx5 molecule shows that both of the solutions that would be equivalent to those presented in Figure 4(c) are lower in rank and have a smaller cluster size than the wild-type. The highest ranking solutions, with larger cluster sizes, predict a docking to Nfs1 of the Grx5 surface that is opposite to Grx5's active center (Fig. 5). An indirect method of testing our docking predictions is by following the protocol previously reported²³ for Glu56 → Arg or Asp88 → Arg Grx5 mutants and studying how cell lines with the wild-type proteins replaced by these two mutants would behave. Then it is necessary to perform the corresponding experiments for Nfs1 and create the point mutants Lys198 → Glu, Arg205 → Glu and Asn141 → Glu. If

the phenotype of the cells subjected to the same types of stress as those in refs. 2, 23 and 29 is similar to the phenotype of the $\Delta grx5$ mutant, this would support our docking predictions.

In addition, we investigated the possibility that Grx5 acts on a dead-end complex formed between Nfs1 and the scaffold proteins Isu1 or Isu2. This complex was obtained in the following way. We knew the residues involved in complex formation in *E. coli* (Cys328 of the Nfs1 homologue and Cys63 of the Isu homologue,⁵² corresponding to Cys421 of Nfs1 and Cys69 of Isu1 and Cys61 of Isu2, respectively). Therefore, we performed docking between Nfs1 and Isu1 or Isu2, constraining the scan in such a way that the Cys residue of Nfs1 and the Cys residue of the scaffold protein would not be at a larger distance than that of a standard disulfide bond. We then studied the docking of Grx5 to the resulting complexes. We found, among the best complexes, configurations in which the three Cys residues are located in close proximity in both the Nfs1–Isu1–Grx5 complex and the Nfs1–Isu2–Grx5 complex (Fig. 4).

Discussion

Although the biochemistry of Grx5 has been characterized, experimental information that clearly identifies the role of Grx5 in FeSC assembly is not yet available, although several studies on the subject have been published.^{30,31,53,54} Some preliminary attempts to determine protein interactions between Grx5 and other FeSC-synthesis proteins by two hybrid assays are underway.⁵⁵ Nevertheless, early biochemical characterization of Grx5^{22,23} has revealed that this molecule may be able to regulate the glutathionylation state of cysteine residues in proteins. In FeSC assembly, cysteine residues are fundamental, both in coordinating the FeSC in the proteins and in the active center of enzymes that catalyze the *de novo* synthesis and repair of FeSC. *In vivo*, it has been known for some time that spontaneous glutathionylation of cysteine residues can regulate protein activity.^{56–58} Therefore, it is clearly possible that Grx5 could be involved in regulating the activity of this pathway via its influence on the glutathionylation state of FeSC biosynthetic proteins.

Due to the non-linearity of the rate laws corresponding to many of the reactions in FeSC assembly,²² the adequacy

Fig. 4. Predicted docking complexes for Grx5. (a) Best docking configuration of Nfs1 (yellow, Cys 421), Isu1 (red, Cys69) and Grx5 (green, Cys60). All of the important Cys residues are in close proximity to each other. (b) Best docking configuration of Nfs1 (yellow, Cys421), Isu2 (red, Cys61) and Grx5 (green, Cys60). All of the important Cys residues are in close proximity to each other. (c) Alternative docking configurations for Nfs1 (yellow) and Grx5 (red). These represent approximately the same docking configuration with respect to either of the Nfs1 monomers in the dimer. The active center Cys60 from Grx5 binds close enough to the putative active center Cys421 of Nfs1 in either. This suggests that Grx5 could act to regulate the glutathionylation state of the Cys421 residue.

Fig. 5. Comparison of the predicted dockings of the mutant forms of Nfs1 and Grx5 to the wild-type of the other. Nfs1 is colored dark yellow, the wild-type docked complex is shown in gray, the docking of Grx5_{Glu56→Arg} to wild-type Nfs1 is shown in red, the docking of Grx5_{Asp88→Arg} to wild-type Nfs1 is shown in green and the docking of mutated Nfs1 to wild-type Grx5 is shown in light yellow and blue.

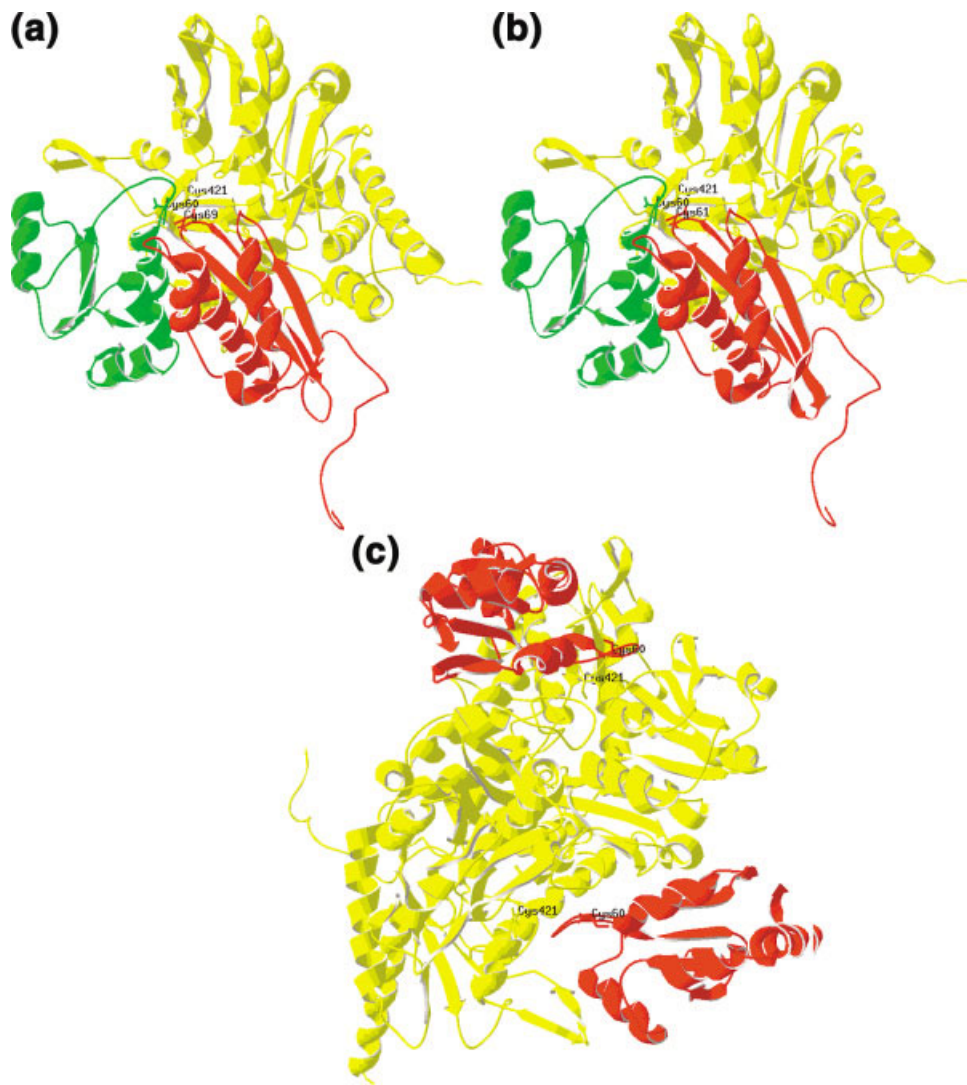


Figure 4.

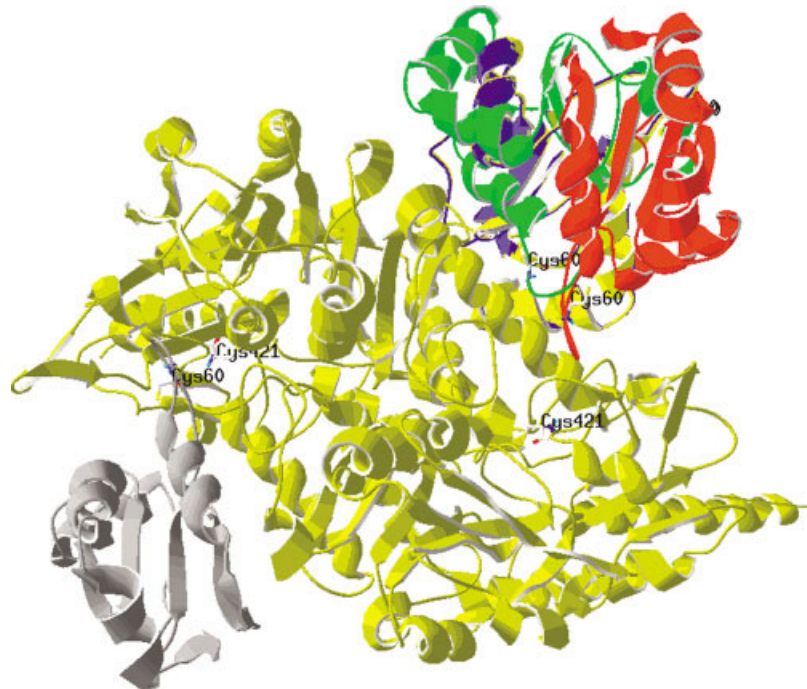


Figure 5.

of the resulting conceptual model in justifying experimental results needs to be tested using quantitative methods based on mathematical systemic modeling. This approach is necessary because a common-sense-based distinction between alternative models supported exclusively by a correlation between two observable quantities in a non-linear process is not guaranteed to be accurate. One can argue that, as is the case here, no accurate estimates for the parameter values of the system are available for deriving a useful mathematical model, and this makes the mathematical modeling impossible. However, by using the power-law formalism as a modeling framework and by normalizing the equations and studying the steady-state or dynamic behavior of the model for large intervals of its parameter values, we may be able to determine the qualitative behavior that is most common to alternative network models. Use of this low-resolution modeling approach has been helpful in discerning distinct roles for proteins in alternative cellular networks.^{21,50,51}

In the case of Grx5, the most immediate question is whether the direct action of Grx5 on FeSC synthesis proteins according to what is known about the biochemical activity of Grx5²² is sufficient to explain the phenotypes that are observed in Grx5-depleted mutants.^{2,23,29} If, after appropriately considering all of the alternative modes of action of Grx5 on FeSC assembly proteins, one cannot reproduce the experimental results, this would be a clear indication that Grx5 action on proteins that are not directly involved in FeSC synthesis is important in explaining its physiological role.

A previous experimental study³⁰ has found that Grx5 depletion leads to the accumulation of FeSC in the scaffold proteins. This has been interpreted as suggesting that Grx5 acts on FeSC after the assembly of FeSC in the scaffold proteins. Our simulations show that this needs not be so. This accumulation, albeit transient, is found upon depletion of Grx5, independent of the mode of action of the protein. Furthermore, our simulations show that if Grx5 acts to regulate the activity of the cysteine desulfurase, Nfs1, the experimental effects of Grx5 depletion on FeSC-dependent enzyme activity and mitochondrial iron accumulation can be qualitatively reproduced, independent of the tested parameter values. This regulation could be achieved by glutathionylating/deglutathionylating Cys residues or by recovering Nfs1–Isu complexes that have been shown to occur at least *in vitro*. If exclusive action of Grx5 on Isu or Arh1 or Yah1 proteins is considered, the dynamic behavior of the resulting mathematical model should not reproduce the iron accumulation and the decrease of FeSC-dependent enzyme activity caused by Grx5 depletion *in vivo*. This indicates that the direct action of Grx5 on Nfs1 or on Nfs1-scaffold protein dead-end complexes may be sufficient to explain the experimental results. Experiments to test this activity could be performed as follows:

(1) Mix isolated and glutathionylated (oxydized) Nfs1 with reduced Grx5 and determine whether Nfs1 becomes more reduced.

(2) Mix isolated Nfs1-scaffold protein dead-end complexes with reduced Grx5 and determine whether indi-

vidual Nfs1 and scaffold proteins appear as a result of Grx5 action.

Additional protein docking studies, using different methods, predict the most likely complexes between Grx5 and Nfs1 as several different alternatives in which the active center Cys60 of Grx5 docks facing the Nfs1 pocket that harbors the Cys421 residue and putative active center cysteine. A set of experiments similar to those performed for Grx5²³ should be undertaken for the cysteine desulfurase Nfs1 in order to evaluate our docking results. Sequence and structural comparison of Nfs1 with the *E. coli* homologue IscS indicates that residue Cys421, which aligns with the active center Cys328 of IscS, is part of the putative active center cysteine in Nfs1. This residue is also predicted to be fairly accessible to the solvent and thus to regulation of activity by glutathionylation/deglutathionylation. Additional docking of Grx5 to putative Nfs1-scaffold protein complexes further supports a possible action of Grx5 on Nfs1 activity. Grx5 is predicted to bind the Nfs1-scaffold protein complexes in a configuration in which the cysteines relevant to protein activity recovery are in close proximity.

Results presented this and the previous article of this series illustrate the usefulness of mathematical modeling as a complementary tool for testing hypotheses about the roles of different proteins involved in a given process. Obviously, the problem is not yet totally solved and new experiments will provide novel insights. In that sense, it would be convenient to provide a way of using the models to explore the meaning of new observations. In the next paper in this series⁵⁹ we plan to present, in addition to our continuing analysis of the individual proteins roles in FeSC biosynthesis, an interactive website where the FeSC community will be able to find and use our results as well as contribute their own experimental results that can challenge our models. This would help in building a database and in suggesting further theoretical experiments to be performed, thus allowing an iterative approach that we predict to be beneficial to the actual development of the field.

ACKNOWLEDGMENTS

We thank Dr. Armindo Salvador and an anonymous reviewer for suggestions on earlier versions of this paper. R. A. was supported by fellowships from the Spanish Ministerio de Educacion, Cultura y Deporte (SB2000-031) and the Portuguese FCT (BPD 11533/2002).

REFERENCES

1. Frazzon J, Fick JR, Dean DR. Biosynthesis of iron-sulphur clusters is a complex and highly conserved process. *Biochem Soc Trans* 2002;30:680–685.
2. Rodriguez-Manzanque MT, Tamarit J, Belli G, Ros J, Herrero E. Grx5 is a mitochondrial glutaredoxin required for the activity of iron/sulfur Enzymes. *Mol Biol Cell* 2002;13:1109–1121.
3. Kim R, Saxena S, Gordon DM, Pain D, Dancis A. J-domain protein, Jac1p, of yeast mitochondria required for iron homeostasis and activity of Fe-S cluster proteins. *J Biol Chem* 2001;276:17524–17532.
4. Lutz T, Westermann B, Neupert W, Herrmann JM. The mitochondrial proteins Ssq1 and Jac1 are required for the assembly of iron sulfur clusters in mitochondria. *J Mol Biol* 2001;307:815–825.

5. Schilke B, Voisine C, Beinert H, Craig E. Evidence for a conserved system for iron metabolism in the mitochondria of *Saccharomyces cerevisiae*. Proc Natl Acad Sci USA 1999;96:10206–10211.
6. Voos W, Röttgers K. Molecular chaperones as essential mediators of mitochondrial biogenesis. Biochim Biophys Acta 2002;1592:51–62.
7. Voisine C, Cheng YC, Ohlson M, Schilke B, Hoff K, Beinert H, Marszalek J, Craig EA. Jac1, a mitochondrial J-type chaperone, is involved in the biogenesis of Fe/S clusters in *Saccharomyces cerevisiae*. Proc Natl Acad Sci USA 2001;98:1483–1488.
8. Kispal G, Csere P, Guiard B, Lill R. The ABC transporter Atm1p is required for mitochondrial iron homeostasis. FEBS Lett 1998;418:346–350.
9. Kispal G, Csere P, Prohl C, Lill R. The mitochondrial proteins Atm1p and Nfs1p are essential for biogenesis of cytosolic Fe/S proteins. EMBO J 1999;18:3981–3989.
10. Mühlenhoff U, Richhardt N, Gerber J, Lill R. Characterization of iron-sulfur protein assembly in isolated mitochondria. A requirement for ATP, NADH, and reduced iron. J Biol Chem 2002;277:29810–29816.
11. Lange H, Kaut A, Kispal G, Lill R. A mitochondrial ferredoxin is essential for biogenesis of cellular iron-sulfur proteins. Proc Natl Acad Sci USA 2000;97:1050–1055.
12. Li J, Saxena S, Pain D, Dancis A. Adrenodoxin reductase homologue (Arh1p) of yeast mitochondria required for iron homeostasis. J Biol Chem 2001;276:1503–1509.
13. Garland SA, Hoff K, Vickery LE, Culotta VC. *Saccharomyces cerevisiae* ISU1 and ISU2, members of a well-conserved gene family for iron-sulfur cluster assembly. J Mol Biol 2000;294:897–907.
14. Jensen LT, Culotta VC. Role of *Saccharomyces cerevisiae* ISA1 and ISA2 in iron homeostasis. Mol Cell Biol 2000;20:3918–3927.
15. Kaut A, Lange H, Diekert K, Kispal G, Lill R. Isa1p is a component of the mitochondrial machinery for maturation of cellular iron-sulfur proteins and requires conserved cysteine residues for function. J Biol Chem 2000;275:15955–15961.
16. Pelzer W, Mühlenhoff U, Diekert K, Siegmund K, Kispal G, Lill R. Mitochondrial Isa2p plays a crucial role in the maturation of cellular iron-sulfur proteins. FEBS Lett 2000;476:134–139.
17. Li J, Kogan M, Knight SA, Pain D, Dancis A. Yeast mitochondrial protein, Nfs1p, coordinately regulates iron-sulfur cluster proteins, cellular iron uptake, and iron distribution. J Biol Chem 2000;274:33025–33034.
18. Duby G, Foury F, Ramazzotti A, Herrmann J, Lutz T. A non-essential function for yeast frataxin in iron-sulfur cluster assembly. Hum Mol Genet 2002;11:2635–2643.
19. Mühlenhoff U, Richhardt N, Ristow M, Kispal G, Lill R. The yeast frataxin homolog Yfh1p plays a specific role in the maturation of cellular Fe/S proteins. Hum Mol Genet 2002;11:2025–2036.
20. Lange H, Lisowsky T, Gerber J, Mühlenhoff U, Kispal G, Lill R. An essential function of the mitochondrial sulphhydryl oxidase Erv1p/ALR in the maturation of cytosolic Fe/S proteins. EMBO Rep 2001;2:715–720.
21. Alves R, Herrero E, Sorribas A. Predictive reconstruction of the mitochondrial iron-sulphur cluster assembly metabolism. I. The role of the protein pair ferredoxin/ferredoxin reductase (Yah1/Arh1). Proteins Struct Funct Bioinformatic 2004;56:354–366.
22. Tamarit J, Belli G, Cabisco E, Herrero E, Ros J. Biochemical characterization of yeast mitochondrial Grx5 monothiol glutaredoxin. J Biol Chem 2003;278:25745–25751.
23. Belli G, Polaina J, Tamarit J, De La Torre MA, Rodriguez-Manzanque MT, Ros J, Herrero E. Structure-function analysis of yeast Grx5 monothiol glutaredoxin defines essential amino acids for the function of the protein. J Biol Chem 2002;277:37590–37596.
24. Herrero E, Ros J. Glutaredoxins and oxidative stress defense in yeast. Methods Enzymol 2002;348:136–146.
25. Holmgren A. Thioredoxin and glutaredoxin systems. J Biol Chem 1989;264:13963–13966.
26. Holmgren A, Aslund F. Glutaredoxin. Methods Enzymol 1995;252:283–292.
27. Savageau MA. Biochemical systems analysis II. The steady state solution for an n-pool system using a power law approximation. J Theor Biol 1969;25:370–379.
28. Shiraishi F, Savageau MA. The tricarboxylic acid cycle in *Dyctios-telium discoideum* II. Evaluation of model consistency and robustness. J Biol Chem 1992;267:22919–22925.
29. Rodriguez-Manzanque MT, RJCESAaHE. Grx5 glutaredoxin plays a central role in protection against protein oxidative damage in *Saccharomyces cerevisiae*. Mol Cell Biol 1999;19:8180–8190.
30. Mühlenhoff U, Gerber J, Richhardt N, Lill R. Components involved in assembly and dislocation of iron-sulfur clusters on the scaffold protein Isu1p. EMBO J 2003;22:4815–4825.
31. Belli G, Polaina J, Tamarit J, De La Torre MA, Rodriguez-Manzanque MT, Ros J, Herrero E. Structure-function analysis of yeast Grx5 monothiol glutaredoxin defines essential amino acids for the function of the protein. J Biol Chem 2002;277:37590–37596.
32. Moul J, Fidelis K, Zemla A, Hubbard T. Critical assessment of methods of protein structure prediction (CASP), round IV. Proteins Struct Funct Genetics 2002;45:2–7.
33. See also <http://predictioncenter.lnl.gov/casp5/pubResultS/>.
34. Bates PA, Kelley LA, MacCallum RM, Sternberg MJE. Enhancement of protein modelling by human intervention in applying the automatic programs 3D-JIGSAW and 3D-PSSM. Proteins Struct Funct Genetics 2001;45:39–46.
35. Guex N, Peitsch MC. SWISS-MODEL and the Swiss-PdbViewer, an environment for comparative protein modeling. Electrophoresis 1997;18:2714–2723.
36. Schwede T, Diemand A, Guex N, Peitsch MC. Protein structure computing in the genomic era. Res Microbiol 2000;151:107–112.
37. <http://calliope.gs.washington.edu/software>.
38. Thompson JD, Higgins DG, Gibson TJ. CLUSTAL W. Improving the sensitivity of progressive multiple sequence alignment through sequence weighting, position-specific gap penalties and weight matrix choice. Nucleic Acids Res 1994;22:4673–4680.
39. Brocchieri L, Karlin S. A symmetric-iterated multiple alignment of protein sequences. J Mol Biol 1998;276:249–264.
40. Westbrook J, Feng Z, Chen L, Yang H, Berman HM. The protein data bank and structural genomics. Nucleic Acids Res 2003;31:489–491.
41. Weiner SJ, Kollman PA, Case DA, Singh UC, Ghio C, Alagona G, Profeta S, Weiner PK. A new force field for molecular mechanical simulation of nucleic acids proteins. J Am Chem Soc 1984;106:765–784.
42. Halperin I, Buyong M, Wolfson H, Nussinov R. Principles of docking, an overview of search algorithms and a guide to scoring functions. Proteins Struct Funct Genetics 2002;47:409–443.
43. Smith GR, Sternberg MJE. Prediction of protein-protein interactions by docking methods. Curr Opin Struct Biol 2002;12:28–35.
44. Tovchigrechko A, Wells CA, Vakser IA. Docking of protein models. Protein Sci 2002;11:1888–1896.
45. Vakser IA. Low-resolution docking, prediction of complexes for undetermined structures. Biopolymers 1996;39:455–464.
46. Vakser IA. Evaluation of GRAMM low-resolution docking methodology on hemagglutinin-antibody complex. Proteins, Struct Funct Genetics 1997;29:226–230.
47. Ritchie DW. Evaluation of protein docking predictions using Hex 3.1 in CAPRI rounds 1 and 2. Proteins Struct Funct Genetics 2003;52:98–106.
48. Tamarit J, Belli G, Cabisco E, Herrero E, Ros J. Biochemical characterization of yeast mitochondrial Grx5 monothiol glutaredoxin. J Biol Chem 2003;278:25745–25751.
49. Nuth M, Yoon T, Cowan JA. Iron-sulfur cluster biosynthesis: characterization of iron nucleation sites for assembly of the [2Fe-2S]²⁺ cluster core in IscU proteins. J Am Chem Soc 2002;124:8774–8775.
50. Alves R, Savageau MA. Extending the method of mathematically controlled comparison to include numerical comparisons. Bioinformatics 2000;16:786–798.
51. Battogtokh D, Asch DK, Case ME, Arnold J, Schuttler HB. An ensemble method for identifying regulatory circuits with special reference to the *qa* gene cluster of *Neurospora crassa*. Proc Natl Acad Sci USA 2002;99:16904–16909.
52. Kato S-I, Mihara H, Kurihara T, Yasuhiro Takahashi Y, Tokumoto U, Yoshimura T, Esaki N. Cys-328 of IscS and Cys-63 of IscU are the sites of disulfide bridge formation in a covalently bound IscS:IscU complex: implications for the mechanism of iron-sulfur cluster assembly. Proc Natl Acad Sci USA 2002;99:5948–5952.
53. Rodriguez-Manzanque MT, Ros J, Cabisco E, Sorribas A, Herrero E. Grx5 glutaredoxin plays a central role in protection against protein oxidative damage in *Saccharomyces cerevisiae*. Mol Cell Biol 1999;19:8180–8190.
54. Rodriguez-Manzanque MT, Tamarit J, Belli G, Ros J, Herrero E.

- Grx5 is a mitochondrial glutaredoxin required for the activity of iron/sulfur enzymes. *Mol Biol Cell* 2002;13:1109–1121.
55. Vilella F, Alves R, Rodriguez-Manzanque MT, Belli G, Swaminathan S, Sunnerhagen P, Herrero E. Evolution and cellular function of monothiol glutaredoxins: involvement in iron-sulphur cluster assembly. *Comp Funct Genom* 2004;5:328–341.
 56. Ghezzi P, Bonetto V. Redox proteomics: identification of oxidatively modified proteins. *Proteomics* 2003;3:1145–1153.
 57. Huang KP, Huang FL. Glutathionylation of proteins by glutathione disulfide S-oxide. *Biochem Pharmacol* 2003;64:1049–1056.
 58. Nulton-Persson AC, Starke DW, Mieyal JJ, Szveda LI. Reversible inactivation of alpha-ketoglutarate dehydrogenase in response to alterations in the mitochondrial glutathione status. *Biochemistry* 2003;42:4235–4242.
 59. Voit EO, Ferreira AEN. Computational analysis of biochemical systems, a practical guide for biochemists and molecular biologists. 2000. Cambridge University Press, Cambridge, UK.
 60. Mendes P. Biochemistry by numbers, simulation of biochemical pathways with Gepasi 3. *Trends Biochem Sci* 1998;22:361–363.
 61. Savageau MA. Biochemical systems analysis II. The steady state solution for an n-pool system using a power law approximation. *J Theor Biol* 1969;25:370–379.
 62. Voit EO, Savageau MA. Accuracy of alternative representations for integrated biochemical systems. *Biochemistry* 1987;26:6869–6880.

APPENDIX: DERIVATION OF MATHEMATICAL MODEL AND PARAMETER SCANNING PROCEDURE

Mathematical Model

The system of ordinary differential equations (SODE) that represents the network in Table I is the following:

$$\begin{aligned}
 dIsu/dt &= v1 + v2 + v3 + v4 + v22 + v23 + v25 + v26 + v27 - v5 - v29 + v30 - v39 + v40 \\
 dIsuFe_1S_1/dt &= v5 + v7 - v1 - v2 - v3 - v6 - v22 - v23 - v26 \\
 dIsuGS/dt &= v30 - v29 \\
 dIsuFe_4S_4/dt &= -dIsu/dt - dIsuGS/dt - dIsuFe_2S_2/dt \\
 dApoP2/dt &= v8 + v24 - v4 - v22 - v35 + v36 \\
 dP2Fe_2S_2/dt &= v22 - v23 - v24 \\
 dP2GS/dt &= v35 - v36 \\
 dP2/dt &= v4 + v9 + v23 - v10 \\
 dP2_I/dt &= -dP2GS/dt - dApoP2/dt - dP2/dt - dP2Fe_2S_2/dt \\
 dApoP1/dt &= v11 - v2 - v33 + v34 \\
 dP1/dt &= v2 + v12 - v13 \\
 dP1GS/dt &= v33 - v34 \\
 dP1_I/dt &= -dP1GS/dt - dApoP1/dt - dP1/dt \\
 dApo_AY1/dt &= v28 - v3 - v31 + v32 \\
 dAY1/dt &= v3 + v14 - v15 \\
 dAY1GS/dt &= v31 - v32 \\
 dAY1_I/dt &= -dAY1GS/dt - dApo_AY1/dt - dAY1/dt \\
 dNfs1/dt &= v38 + v40 - v37 - v39 \\
 dNfs1GS/dt &= v37 - v38 \\
 dNfs1_Isu/dt &= v39 - v40 \\
 dFe/dt &= v16 + v17 + 2(v1 + v7 + v11 + v24 + v28) + 4(v8 + v25) - v18 - v19 - 2(v5 + v6) \\
 dHeme/dt &= v17 + v20 - v19 - v21
 \end{aligned}$$

$$\begin{aligned}
 dHeme_Fe/dt &= v19 - v17 \\
 dGrx5/dt &= -v41
 \end{aligned}$$

Each v_i ($1 \leq i \leq 28$) is given in detail in Table I. Each reaction is expressed as a power-law term according to well-established rules. For a detailed derivation of the equations, see the appendix to the previous paper in this series.²¹ Numerical solution of SODE in our work was completed using the programs PLAS⁵⁹ and GEPASI.⁶⁰

Parameter Scanning Procedure

The 41 rate constants in our model are positive. Because no inhibitory feedback is involved in any of the considered reactions, all 52 kinetic orders are non-negative. The available data do not allow the determination of actual concentrations and absolute rates for many of the processes we need to consider. However, they do allow for the estimation of relative rates with respect to normal steady-state values of the different molecular species being considered. The same is true for the kinetic orders. Thus, by normalizing the equations with respect to standard steady-state values of the variable, we are able to study the qualitative behavior of the model. The basal values for rate constants and kinetic orders are given in the previous paper of this series.²¹

Parameter scanning was completed as follows. Kinetic orders have values that are bound by small integer numbers (between 0 and 5 in absolute value^{61,62}). We assumed that the kinetic order of Grx5 in every reaction in which it is considered to participate is the same due to the similarity of the processes. Thus, we ran 540 different simulations to account for all possible combinations of Grx5 action generated by Table II. Because our estimates of rates came from experiments by different groups, under different conditions and sometimes using different systems, we also sampled the ratios between different relative rates. We sampled the ratio between the rate of *de novo* synthesis of FeSC and the rate of FeSC *in situ* repair, the rate of FeSC transfer to the cytoplasm and the ratio of Heme_Fe to FeSC synthesis, taking independent samples at different values for each of the ratios (0.001, 0.01, 0.1, 1, 10, 100). Additionally, we repeated this experiment allowing for the possibility that Arh1 does not act on FeSC through Yah1 ($\alpha3 = \alpha14 = \alpha15 = \alpha28 = 0$). Compounding this scanning with that for the rate constant of Grx5 action (0.001, 0.01, 0.1, 1, 10, 100), we calculated a total of approximately 38000 time curves of Grx5 depletion, allowing each simulation to run until the amount of Grx5 was no larger than 10^{-10} . We evaluated by visual inspection which curves reproduced the expected phenotype of deficient FeSC-dependent enzyme activity and mitochondrial iron accumulation.